Towards the automation of the die spotting process: Contact blue pattern decryption

Alaitz Zabala *, Iñigo Llavori, Eneko Sáenz de Argandoña, Joseba Mendiguren

Mechanical and Industrial Manufacturing Department, Mondragon Unibertsitatea, Loramendi 4, 20500, Mondragón, Spain

ARTICLE INFO

ABSTRACT

Automotive die spotting is one of the most complex and least standardized processes in the tool making process. A spotting expert identifies local contact areas through a blue-paste pattern and the die/sheet contact is optimized by manual grinding. Research performed on the impact of tribology conditions and surface irregularities on die behaviour have demonstrated the critical importance of die/sheet contact. Therefore, correctly understanding, standardizing, and automatizing die spotting is of a great interest for the industry. In this work, the first step toward the die spotting automation is performed by decrypting the contact blue pattern. Different test procedures were followed in order to decrypt the relation between the blue-paste pattern and the contact pressure and gap appearance in the interface. Additionally, a numerical method for automatic contact pressure detection based on the blue pattern was developed and validated. The outcome of this study is presented as potential tool for objective decision making towards the automation of the die spotting process and die contact analysis, focused to decrease try-out loops and thus reducing production time and costs.

1. Introduction

In the last half century, the automotive industry has been on the forefront of standardization, mass production, and manufacturing efficiency. One passenger vehicle is the combination of around 30,000 individual components. The main structural part of the car is called the body in white (BIW). The BIW consists of the various components of the car body joined together (e.g., by welding), which composes the framework upon which the rest of the car is mounted. It is estimated that, on average, the BIW comprises up to the 28 % of the car's weight [1]. The main manufacturing process used for BIW components is the stamping/drawing metal forming process. As stated by Ficko et al. [2] the low cost of the manufacturing and maintenance of these process makes the technology ideal for mass-produced products.

For most in-die manufacturing processes, die cost has a critical impact on the final product cost. Therefore, an important effort has been made in the last few decades to reduce the cost/lead time of automotive die manufacturing. A clear example of this trend is the study of Schuh et al. [3] on the impact of the cutting manufacturing failure on the cost of the tooling. It is estimated that an average lead time of 25 months is necessary to produce a die, which includes engineering, manufacturing, and try-out phases. Birkert et al. [4] estimated that on its own, this last

phase (try-out) consumes around six months and 32 % of the die cost. That is why numerous investigations have been conducted in order to increase the accuracy of the engineering phase and thus reduce the try-out phase duration.

Multiple investigations have been carried out to identify better algorithms to predict the forming outcome, with some cases even exploring the use of genetic algorithms, as the work of Wei et al. [5] in where an springback control of a cylinder shallow shell was developed using reponse-surface methods and multi-objective genetic algorithms. As the sheet material behaviour is one of the key elements involved in forming performance, the phenomena involved in the correct modelling of this behaviour has been widely researched in the last few decades. Among the numerous effects studied, the non-linearity of the elastic in spring-back predictions, studied for example by Mendiguren et al. [6] for the TRIP700 steel; the complex plastic flow of highly textured materials collected by Banabic [7] in his book; and the complexity of the failure under the necking modulus can be highlighted. A clear example of the former is the dependency of the necking limit to the bending strains investigated by Neuhauser et al. [8] for DP600 material.

One effect that had been long overlooked but has been gaining increased attention in the last few years is the impact of die/sheet interface tribological behaviour on the performance of the forming

---

process. Multiple investigations have been carried out to investigate this phenomenon [9,10].

On the one hand, industrial component-based research has been carried out by applied scientists. Sigvant et al. analysed accuracy improvements made when simulating the drawing process of a Volvo XC90 inner door based on the dependency of the friction coefficient on the contact pressure, the sliding velocity, and sheet deformation. The friction coefficient was numerically calculated in a range of pressures between 0 MPa and 50 MPa, and variations between 0.18 and 0.11 were found. As a result of the study, a strong influence of the tribological and friction conditions on both the quality of the inner door and the overall production stability was concluded. The simulated draw-in results were strongly dependent on both an accurate description of the friction and a geometrical description of the actual tools and draw-beads [11].

In a second study, Tatipala et al. [12] analysed the process robustness on a simulation of forming of the Volvo XC90 inner door. Among the different variables they studied, the blank holding pressure was found to be one of the key aspects. In addition, they concluded that, in order to achieve the correct representation of the local contact points, it was necessary to scan the surfaces of the real dies in order to be able to calculate the real distances between the blank holder and the die. This was found to have a critical impact on the pressure distribution and therefore on the material flow restriction behaviour.

Later, Sigvant et al. [13] extended the analysis to include the influence of surface roughness and strain rate on the simulations, incorporated analysing its impact on the tribological behaviour changes. When analysing the sheet material of VDA239 CR4 GI and the die material of GGG70 L, a decrease of 0.1 in the friction coefficient between the pressures of 2 MPa and 35 MPa was reported.

On the other hand, more fundamental research works have also been conducted in order to understand the mechanics behind the tribological pair. Merklein et al. [14] explored the possibility of a dry condition sheet metal forming processes. In order to do so, they investigated the tribological behaviour between dies of 1.2379 and sheet material of DC04. They analysed dies with roughness values between 0.04 and 0.45 μm of Ra under contact pressures of 1 MPa, emulating the blank holding area, while Arumugaprabu et al. [15], in a review, summarized the importance of the surface texturing of materials to improve their tribological performance.

Aiming at developing a tool for further enhancing understanding and the tribological pair, Shisode et al. [16] recently developed a semi-analytical contact model to determine the flattening behaviour of coated sheets under normal pressure.

Pilthammar et al., in two consecutive works, studied the impact of die/press deflection on the contact behaviour between the blank-holder and die as well as how these could critically impact the results of the forming process. In their first work in 2017, they studied die surface deflection stemming from this effect [17], while in their second study, they analysed the possible improvement introduced by virtual spotting [18]. As described by Pilthammar and co-workers, spotting is a technique in which the metal sheet is painted (with a special blue paste) before the die is closed, and when the die is opened, the contact areas can be identified as the areas in which a paint transfer from the sheet to the die (and blank holder) has taken place. It is a common belief within the tool-making industry that the blue paste pattern allows for the identification of different contact behaviours, ranging from 'very soft contact' to 'very hard contact'. In addition to this, it allows for identifying local areas in which the gap between the sheet surface and the surface of the die are some hundredths of a mm. This will provide the try-out specialist with information regarding where to grind in order to achieve at least the 90 % of contact needed to begin the try-out step.

The importance of the rigidity of the system on contact behaviour was corroborated at the laboratory level by Recklin et al. [19], who investigated the influence of this rigidity by analysing the influence of the test stand and the contact size sensitivity on the friction coefficient in sheet metal forming. They analysed a range of pressures between 2 MPa

and 8 MPa with a sheet material of DX56 D + Z and a tool material of E-JS 2070.

The deflection of the tool directly affects the die/sheet interface local pressure condition and therefore the tribological behaviour. Bolay et al. [20] studied the impact of an improved representation of the effect of friction behaviour on the draw-bead area for the correct prediction of two aluminium fenders formed by correctly considering the bearing zone before the draw-bead. They found that, even at the laboratory level (in which presumably no manual grinding was performed), the local contact area pressures between 15 MPa and 20 MPa were identified on the bead areas with pressures up to 11 MPa on the flat areas. They used numerical simulation, blue spotting paste, and Fujifilm Prescale films in order to perform this evaluation. Following with the same approach, Leocata et al. [21] analysed the behaviour of the material when passing through a draw bead. It was taken into account that, due to the manual grinding performed during the spotting step, as well as the draw bead design, a different localization of the main pressure zone could be achieved. They concluded a critical difference in the behaviour of the forming process depending on the pressure concentration area.

Based on the critical importance of die spotting, Essig et al. [22] presented a digital processing methodology in order to support the toolmaker with blue paste pattern identification. The main aim was to produce digital spotting images in order to generate advance reporting on the contact performance of the die.

From the above review, it is clear that the localization of the contact points is critical in the tribological behaviour of the die and, therefore, the overall performance of the die set. Nowadays, the local modification of the tool surface to compensate for sheet thinning/thickening, die deflection, or even machining irregularities is manually performed by locally grinding during the try-out step. In order to evaluate the contact behaviour, the try-out expert uses the blue paste pattern remaining in the die and sheet surfaces after opening the die. However, the interpretation of the pattern remains a trade secret that is acquired though experience. Although the computer-aided technology is used for tool design [23], there is still not implemented in the try-out step. There are already initiatives, such as the one previously presented by Essig et al., aiming for the automatization of the process; however, the contact blue pattern automatic interpretation is still unknown.

In this work, the first step toward the automatization of spotting was performed via the decryption of the contact blue pattern. In order to do so, different contact conditions (i.e., different apparent pressures and surface irregularities) were analysed by means of blue paste and pressure sensitive films. In addition, an automatic pressure interpretation numerical tool based on the blue patterns is proposed.

2. Materials and specimens

2.1. Samples

Two different contact bodies were used in this study: a strip of AA5754 material with dimensions of $100 \times 50 \times 2$ mm and a strip drawing test block [24] made of GGG70 L material (see Fig. 1). The flat surface of this block was 52×26 mm with rounded edges 5 mm in radius (the radii were not included on the given contact surface).

2.2. Materials

As previously introduced, two different materials were used. On the one hand, an AA5754 sheet material was employed as a material representative of automotive components. The material presents a roughness of Ra = 0.5 ± 0.02 and is characterised by its elastic modulus of 70 GPa, a Poisson ratio of 0.33, an averaged r-value of 0.7, and a yield strength of 130 MPa.

The other die material was a hardened GGG70 with a surface hardness of 260.3 HV (Ra = 0.4 ± 0.03). This is the most commonly used material in automotive outer panel die construction as shown by Sigvant
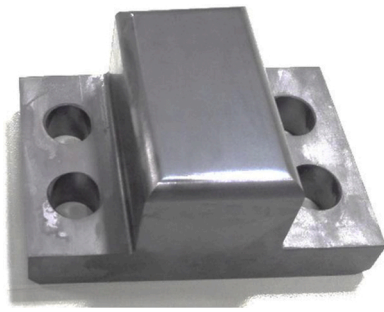
Fig. 1. Image of the die block used for the test.

et al. on their study [13]. The elastic modulus of the die was 176 GPa, with a Poisson ratio of 0.33 and a yield strength of 420 MPa.

2.3. Blue paste

A blue non-drying paste from EGA Company was used in this study. The blue paste was deposited through a painting roll following the same industrial methodology used in automotive die spotting and try-out. A layer of five-μm blue paste was administrated in this study, as it is representative of the industrial standard and has been confirmed on both laboratory and industrial scales by means of a wet film thickness gage following the ASTM 1212−91 standard [25] (Test Method A).

3. Experimental procedure

Three different test procedures were followed in this study. First, flat-on-flat surface contact was analysed to understand the blue paste pattern evolution under increasing contact pressures. Then, the potential transfer of the blue paste under non-contact conditions were studied. To this end, controlled gaps were introduced artificially in the upper and lower interfaces to simulate the surface waviness of real dies. Finally, an irregular contact scenario was analysed in order to validate the obtained conclusions.

3.1. Flat-on-flat contact

The schematic of the test procedure is shown in Fig. 2. First, the lower die was fixed on top of a hard rubber in order to absorb the potential misalignments and assure the best homogeneous contact distribution. Then, the sheet (with the blue paste layer) was placed on top of
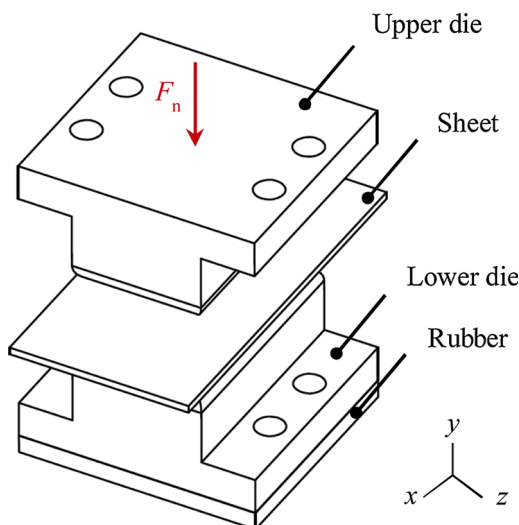

Fig. 2. Schematic of the test configuration.

the lower die. Finally, the top die was positioned above the sheet and mounted in a precision tension-compression machine (INSTRON 4206) to control the movement and force.

In each test, the apparent contact pressure was incrementally increased in order to observe the evolution of the contact pattern through the blue paste technique. Once all bodies were placed (still no contact occurred between the upper die and the sheet), the upper die was pressed gently until the desired contact force was reached (this step took 120 s). Then, the contact force was kept constant for another 120 s to ensure the movement of the blue paste through the contact interface. Finally, the upper die was lifted, and the sheet and die patterns were evaluated (without moving the position of the sheet). Following this procedure, increasing pressure tests were carried out consecutively in order to analyse the blue pattern evolution, summarised in Table 1 (the tests were carried out three times to ensure repeatability, but the results of one series is presented for the sake of simplicity). The apparent contact pressures were calculated by dividing the normal force (accurately controlled by the tension/compression INSTRON 4206) by the theoretical projected contact area of the die (52 mm x 26 mm), (i.e., the effect of the rounded edges was ignored). The pressure range analysed in this work is representative of the pressure distribution found on a drawing tooling [20]. Nevertheless, it should be noted at this point that real contact takes place in localized asperities and protuberances, and, therefore, different true contact pressures can coexist on the surface.

In this test procedure, only the upper surface of the sheet was painted and analysed, since the sheet was kept in the same position between the tests. Accordingly, one interface blue paste contact pattern corresponding to the sheet and die surfaces was reported at each test. The sheet was painted before beginning the test, then the first pressure was analysed. Once the patterns were evaluated, the upper die was moved down to generate the next target pressure (without intermediate re-painting).

3.2. Spaced contact

Based on the introduction and literature review, it can be stated that some authors in the industry are based on the blue paste pattern in order to evaluate the gap between the sheet and die under a specific test condition. The second test procedure of the present study is therefore aimed to analyse the influence of the gap on the interface. In order to study this effect, two different test configurations were analysed: LARGE space and SHORT space (Fig. 3). In both cases, calibrated 10 μm and 20 μm gauge strips were used (ACHA Company) in order to generate controlled protuberances to artificially simulate the influence of the waviness of the real surfaces. This calibrated gauges had a width of 12.7 mm and were positioned to generate two spacings (h), called LARGE and SHORT, with an approximated space between the gauges of 36.4 and 10.6 mm respectively (see Fig. 3). Differing from the previous test procedure, both surfaces of the sheet were painted, and, therefore, the four surfaces (each side of the sheet and the two dies) are reported in the experimental results section.

The tests followed the procedure explained in the flat-on-flat test section, however, in this case the sheet was removed after each test for the two interface analysis. Consequently, the sheet was cleaned, and a new five-μm layer of blue paste was deposited before being placed again on the lower die. In addition, a secondary test under the same test condition was conducted, in which a pressure-sensitive film (Fujifilm Prescale Film) was used instead of the blue paste layer. These films change the colour when pressure is applied on the surface, allowing for the direct observation of the pressure distribution though a red shaded

Table 1
Flat on flat apparent contact pressure values.

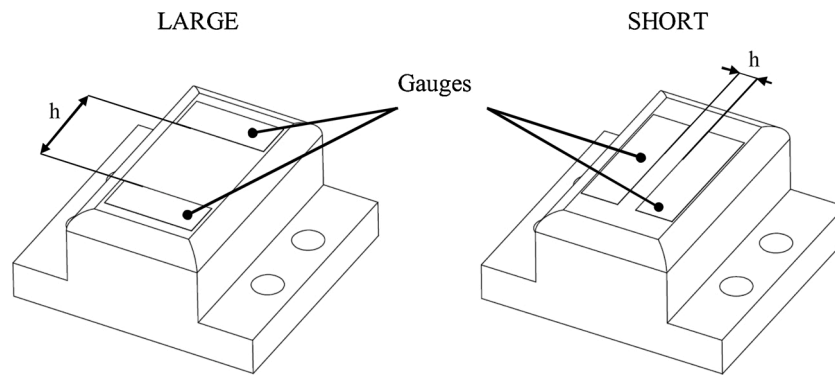| Tests	1st	2nd	3th	4th	5th	6th	7th	8th	9th
Pressure [MPa]	0	0.5	1	2	5	10	15	20	25

Fig. 3. Spaced contact. Both configurations, i.e. LARGE and SHORT, are shown with the distance 'h' between the gauges to be approximately 36.4 mm for the LARGE configuration and around 10.6 mm for the SHORT.

density pattern. Different pressure range films (according to the applied apparent pressures) were used in the study (see Table 2). Similar to the previous test procedure, three tests were conducted for each condition in order to assure repeatability, but only one is presented for the sake of simplicity.

Table 3 summarises the test conditions for this spaced contact test procedure. Protuberances of 10 μm and 20 μm were analysed, and the positioning of the calibrated gauges led to LARGE and SHORT spaces. In addition to this, two different configurations were studied. On the first configuration, the gap was introduced only in the lower interface. On the second configuration, the gap was introduced in both interfaces. Under these spaced test conditions, the two extreme contact pressure conditions analysed in the previous configuration (0.5 MPa and 25 MPa) were studied. Each row of the table represents the two scenarios of each variable. A full factorial of these variables was analysed with three replicates, resulting in a total of 48 tests.

3.3. Irregular contact

In this case, a pair of industrial-flat contact surfaces prior to spotting were analysed. The surfaces were manually polished by a die spotting expert (Ra = 0.66 ± 0.04) in order to resemble the industrial case.

In order to analyse the evolution of the blue paste pattern, only the lower interface was studied. In this case, both surfaces of this interface (die and sheet) were analysed. Tests with increasing pressure were conducted, and blue paste patterns and pressure film patterns were analysed (see Table 4). Similar to the previous test procedure, three tests were conducted for each condition in order to assure repeatability, but only one is presented for the sake of simplicity. In this test procedure, a new blue paste layer was introduced per each pressure test (i.e., sample painting, moving down until target pressure, opening the dies to evaluate the pattern, cleaning the sample, depositing a new blue paste layer, and repeating the process under the next target pressure).

4. Results and discussion

In this section, the experimental data of the three testing strategies (i.e., flat-on-flat contact, spaced contact, and irregular industrial-flat, contact) are presented, and the results are critically discussed.

Table 2
Calibrated range of pressures of the used pressure-films.

Film designation	Apparent contact pressures		
Ultra Super Low Pressure	0.5 MPa	0.5 MPa	
Super Low Pressure	1 MPa	2 MPa	
Low Pressure	5 MPa	8 MPa	10 MPa
Medium Pressure	15 MPa	20 MPa	25 MPa

Table 3
Summary of the "Gap contact" testing procedure details.

Measurement technique	Pressure	Protuberance height	Gap space (h)	Nº of gap interfaces
Blue paste	0.5 MPa	10 μm	LARGE	One
Pressure film	25 MPa	20 μm	SHORT	Both

Table 4
Irregular contact pressure values.

Tests	1st	2nd	3th	4th	5th	6th	7th	8th
Pressure [MPa]	0.5	1	2	5	10	15	20	25

4.1. Flat-on flat contact

Fig. 4 depicts the results corresponding to the flat-on-flat contact tests, during which the evolution of the blue paste on one of the die/sheet interfaces was analysed under increased apparent contact pressure ranging from 0 to 25 MPa. Different trends were identified according to the different applied pressure ranges.

4.1.1. No blue paste transfer from the sheet (0MPa)
The first test was conducted under close to 0 MPa (as soon as the machine detected slight contact, the die was lifted). It should be noted at this point that, even with ground surfaces, the blue paste pattern was able to detect slight differences in flatness (and/or parallelism). This can be observed as a clear contact can be noted on the top left side of the image (see Fig. 4, contact pressure 0 MPa, die part). As expected, the sheet maintained the entire blue paste, while almost nothing was transferred to the die due to the almost absence of contact between the surfaces.

4.1.2. Blue paste transfer from sheet to die (0.5-2 MPa)
When increasing the apparent contact pressure to 0.5 MPa, the first blue paste transfer occurred from the sheet to the die. In addition, it can be clearly observed that the true contact differed from the theoretical apparent contact. The waviness of the surface was readily observable via the blue pattern of the die surface. At one quarter from the top, harder contact than that compared to the rest of the area was observed, at which the blue paste was completely transferred to the die. However, on other areas (e.g. the lower right area), very soft contact (if any) can be noted, as the sheet maintained the blue paste, and almost nothing was transferred to the die. At higher contact pressures (2 MPa), the blue transfer intensity increased in the harder contact areas, at which the sheet started to lose the majority of the blue paste, transferring it to the die surface. In addition to this, speckled areas were observed for the first time. This speckled pattern is the representation of the industrial context
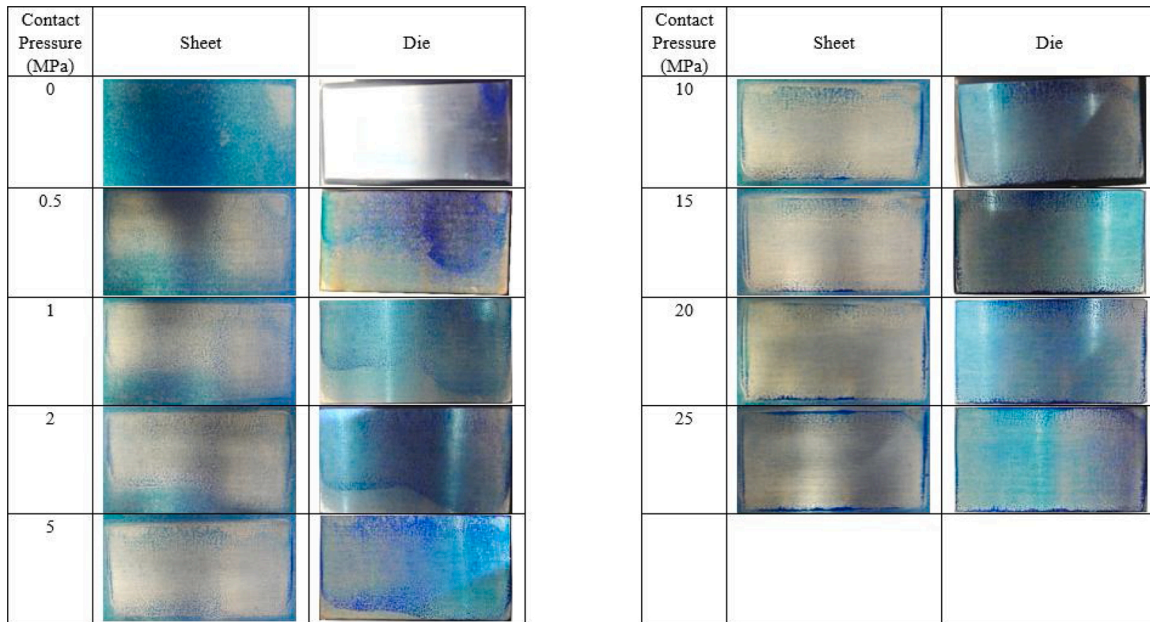
Fig. 4. Analysis of the blue paste evolution on the flat-on-flat sheet-die interface under increasing apparent contact pressures (from 0 MPa to 25 MPa) (For interpretation of the references to colour in this figure legend, the reader is referred to the web version of this article.).

of soft contact. Additionally, it was observed that the true contact area of the 2 MPa test increased considerably from the real contact area observed with the 0.5 MPa test (readily observable with the visual comparison of the blue pattern on the die surfaces of both tests). The lower part of the die that did not present any contact under lower pressure values began to reveal a soft contact (a minimum amount of blue paste was transferred from the sheet to the die).

4.1.3. Blue paste transfer from sheet to die + die losing blue paste (5-15 MPa)

When increasing the contact pressure from 2 MPa to 5 MPa, following the previously identified trend, the sheet kept losing the blue paste. In that case, however, it could be observed that, along with the sheet, the die also started losing the blue paste as well (e.g., central left area). This trend continued with the higher contact pressure tests (e.g., 10, 15 MPa).

4.1.4. Sheet without blue paste (20-25 MPa)

At high apparent contact pressures, the sheet had almost lost all the

blue paste with the exception of its edges, at which a build-up was observed. This build-up presumably came from the blue paste being eliminated from these edges due to the high contact pressure on the interface.

It can be concluded from these tests that the blue paste remained in the sheet as long as there was no contact. When the contact-pressure increased, the blue paste began to transfer from the sheet to the die on the true contact zones (generating different blue shades on the die according to the contact intensity: showing a light blue in the soft contacts and strong blue on the hard contact zones). However, at higher contact pressures, the blue paste was pushed out of the interface, resulting in clean surfaces on both the sheet and die.

Fig. 5 represents the estimated (by visual inspection) evolution of the amount of blue paste (in percentage). Fig. 5a shows the whole analysed range of apparent pressures (0 MPa to 25 MPa), while Fig. 5b shows a zoomed-in view of the 0 MPa to 5 MPa area.

Considering the first events up to 5 MPa (Fig. 5b), it can be observed that a very important blue paste transfer from the sheet to the die already took place under 0.5 MPa apparent contact pressure. From 0.5 to
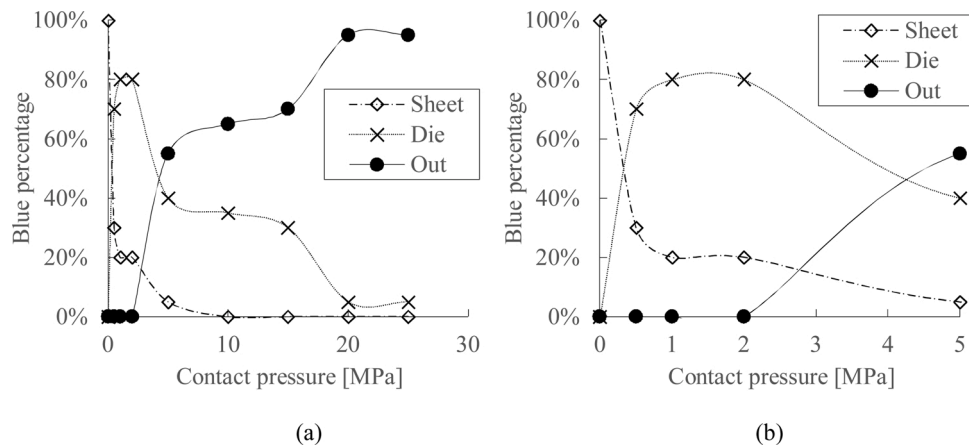

Fig. 5. Estimated evolution of the blue paste percentage on the interface dependent on the contact pressure (out refers to the blue paste squeezed out of the contact area): a) results within the range of 0 MPa to 25 MPa and b) zoomed-in section from 0 MPa to 5 MPa. Note: Estimated values for trend depicting purposes (For interpretation of the references to colour in this figure legend, the reader is referred to the web version of this article.).

5 MPa, the sheet presented a near linear trend in terms of the blue paste decrease. This blue paste was transferred to the die at first (up to 2 MPa) and then was pushed out from the interface, as evidenced by the blue percentage decrease in the die from 2 MPa onward. As can be observed in Fig. 5a, from 20 MPa onward, neither the die nor the sheet retained almost blue paste, which was evacuated from the interface and was computed as 'out'. This trend is schematically presented in Table 5.

4.2. Spaced contact

As presented in the methodology section, the objective of this set of tests was to clarify how, at the industry level, the blue paste pattern is interpreted, not just in terms of the intensity of its contact (soft to hard) but also as a tool for identifying the distance between the interface surfaces for die verification and correction during the die spotting process. To this end, controlled gaps of 10 and 20 μm were located at one interface (one-gap test) or at both interfaces (two-gap test) located at different distances called LARGE and SHORT.

4.2.1. Only one side gap

Fig. 6 summarises the contact patterns (both blue paste and press-sensitive film) of the one-gap LARGE space tests performed under the apparent contact pressure of 0.5 MPa with 10 μm (Fig. 6a) and 20 μm (Fig. 6b) gaps. In these tests, the gaps were located at one of the interfaces, and results corresponding to both interfaces have been reported (gap interface: above; flat interface: below).

Like the flat-on-flat contact configuration, it can also be noted that, even with grinded dies, the contact did not exhibit perfect parallelism, and preferential contact was observed on the bottom side of the die/sheet. This effect could be noted in both tests (10 μm gap Fig. 6a; 20 μm gap Fig. 6b) for the pressure film and blue paste patterns of both interfaces (gap and flat). Considering the gap interface (above), the way in which the blue paste was transferred to the die can be observed for both 10 μm and 20 μm cases, which could be classified as 'medium contact' according to the previously defined classifications (Table 5). In the case of the 10 μm gap test (Fig. 6a), slight contact could be noted in the gap area (centre of the die), since blue paste transfer was observed in the die, and the pressure film presented contact patterns. Examining the sheet image, however, no visual decrease in blue paste amount was observed. Accordingly, this contact could be classified between 'very soft contact' and 'soft contact' (Table 5). It should be noted that this contact in the gap area could not be noted in the same configuration test with a 20 μm gap (Fig. 6b). Considering that the blue paste layer applied to the sheet was 5 μm thick, and the die contact took place in the centre area in the 10 μm gap test, it could be presumed that the sheet deformed locally even if the apparent contact pressure was 0.5 MPa (probably due to the true contact pressures raised from the non-homogenous contact).

From these results, it can be concluded that, even if a non-homogeneous force/local pressure distribution was observed, the increase in the gap height to 20 μm substantially decreased the possible contact in the centre area.

Fig. 7 shows the 10 μm gap (a) and 20 μm (b) results under 0.5 MPa apparent pressure with the SHORT space between the protuberances. In this case, the non-homogeneous force/local pressure distribution was

also observed in both tests, but the short distance between the protuberances did not allow for the material to sufficiently deform to generate contact with the central area.

Following, the results obtained for the same configurations under higher apparent pressures of 25 MPa are presented. Fig. 8 summarises the contact patterns of the one-gap LARGE space tests performed under the apparent contact pressure of 25 MPa with 10 μm (Fig. 8a) and 20 μm (Fig. 8b) gaps.

On the one hand, it can be noted how, under these high pressures, the rubber under the lower die balanced the forces, and a more homogeneous contact distribution was observed (compared to that obtained under 0.5 MPa, Fig. 6). It is clear that the main contact pressure was transmitted though the protuberance areas and had a clear effect on the blue paste patterns in both the gap interface and flat interface. Both surfaces (die and sheet) lost the blue paste with contact on the protuberance areas, which could be classified as 'very hard contact' (Table 5). The local point on the flat interface (also represented in the pressure film pattern) corresponded to a defect in the sheet surface. This defect can also be noted in some of the following figures in this section.

On the other hand, under these high pressures, the deformation of the sheet was accentuated, and a higher contact area occurred at the central part in the 10 μm gap test (Fig. 8a), in which 'medium contact' (Table 5) was observed as the sheet lost the blue paste. In addition, the 'very hard contact' (Table 5) shown in the flat interface pushed the blue paste to the edges, and a clear speckled area can be observed in these zones. In the case of the 20 μm gap test (Fig. 8b), the local deformation of the sheet was not very prominent. Slight contact was observed in the centre, which could be classified as even less than 'very soft contact' (Table 5).

Fig. 9 shows the results corresponding to the 10 and 20 μm gap under 25 MPa when the protuberances had SHORT space between them, decreasing the material's ability to deform.

In the 10 μm gap test (Fig. 9a), it can be noted that the centre part of the gap area presented a contact, as can be observed in the pressure film, which indicates the local deformation of the material. The die gap area boundaries presented a build-up of the blue paste, which probably was pushed out of the protuberance contact due to the strong contact pressure, which could be classified as 'very hard contact' (Table 5), since both the die and sheet lost the blue paste. The centre of the die gap, however, exhibited a very small amount of blue paste, which indicated that the contact on the die centre was between 'very soft' and 'soft' in terms of classification (Table 5). In this case, both the flat contact interface and the right protuberance of the gap contact interface were very 'hard contact' in nature. Similar to that observed in the 0.5 MPa tests, the increase in the gap to 20 μm eliminated contact in the centre area (Fig. 9b).

4.2.2. Gap on both sides

In the previous tests, only one of the interfaces presented gaps, which was pressed against a flat surface. In the following examples, two gap surfaces were facing each other (with the same protuberance distribution and height).

Fig. 10 shows the contact patterns of the sheet between both gap surfaces, with a LARGE space between the gauges of 10 μm (Fig. 10a) and 20 μm (Fig. 10b) under 0.5 MPa apparent pressure. It can be noted how 'soft contact' took place at the protuberance areas without any contact with the central area.

Similarly, when analysing the same configurations (two gap surfaces facing each other) with the SHORT space (Fig. 11), 'very soft contact' could be found on the protuberance area, but no blue paste transfer was found on the central area (the images show a bluish reflex effect of light that does not correspond to blue paste transfer).

Once the contact pressure was increased to 25 MPa, blue paste transfer was observed at the central area under the LARGE space with 10-μm gauges (Fig. 12a). In addition to this, 'hard' to 'very hard' contact (Table 5) can be observed on the gauge area. However, the increase in

Table 5
Flat on flat contact trend.

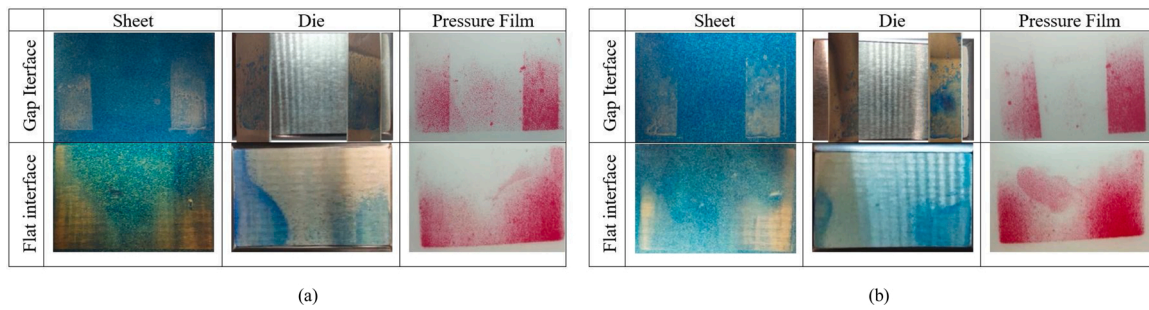| Sheet blue paste pattern	Die blue paste pattern	Local contact pressure	Range of pressure
Strong blue	No blue	Very soft contact	0 MPa – < 0.5 MPa
Light blue	Light blue	Soft contact	0.5 MPa – 1 MPa
Very light blue	Strong blue	Medium contact	2 MPa – 5 MPa
No blue	Light blue	Hard contact	5 MPa – 10 MPa
No blue	No blue	Very hard contact	15 MPa – 25 MPa

Fig. 6. Only one side gap/LARGE space between protuberances of 10 microns (a) and 20 microns (b) under 0.5 MPa of apparent contact pressure.
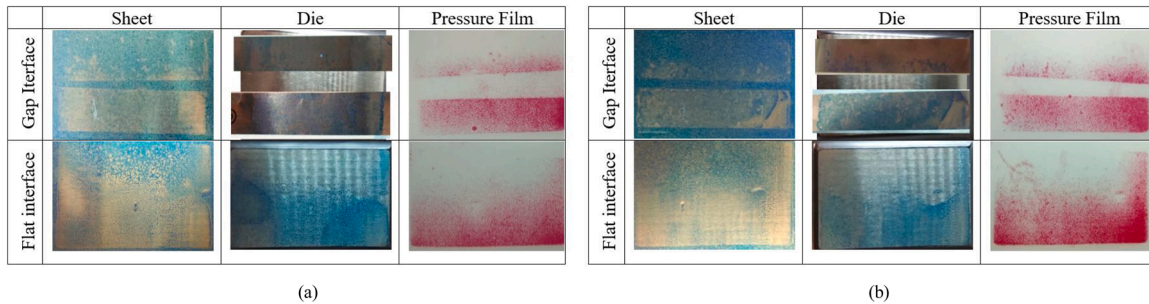

Fig. 7. Only one side gap/SHORT space between protuberances of 10 microns (a) and 20 microns (b) under 0.5 MPa of apparent contact pressure.
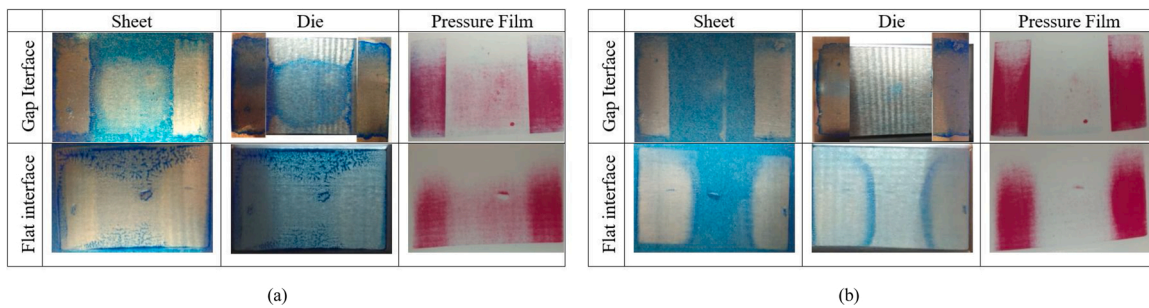

Fig. 8. Only one side gap/LARGE space between protuberances of 10 microns (a) and 20 microns (b) under 25 MPa of apparent contact pressure.
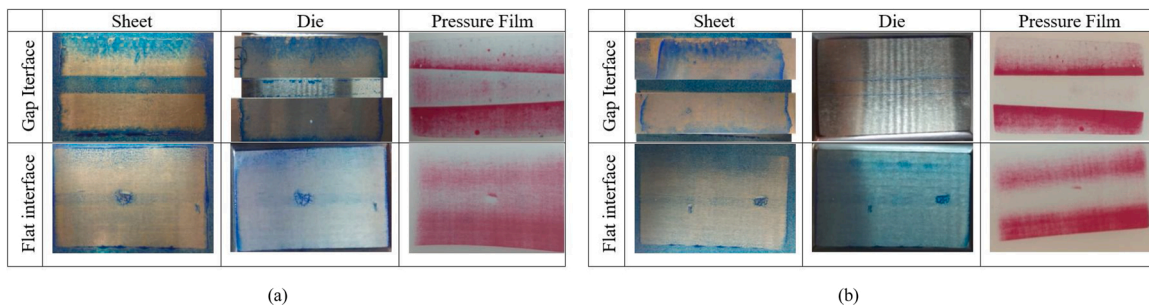

Fig. 9. Only one side gap/SHORT space between protuberances of 10 microns (a) and 20 microns (b) under 25 MPa of apparent contact pressure.

the protuberance height to 20 μm did not allow for the blue paste transfer at the central area (Fig. 12b). As can be observed in Fig. 13, similar results were observed under 25 MPa when reducing the space between the protuberances (SHORT) for both 10 μm and 20 μm protuberance heights.

From these results regarding the patterns of protuberance-based spaced contact, it can be noted that the blue paste pattern did not only depend on the gap but also on the pressure and distance between the gauges (Table 6).

From the obtained results, it can be concluded that central contact ceased once the gap was increased from 10 μm to 20 μm in cases in which only one gap interface and the LARGE space scenario were considered. Under the SHORT space scenario, the apparent pressure of 25 MPa was necessary to generate central contact, which was only possible with gauges of 10 μm. When the gap was considered at both interfaces, and thus less pressure was applied to the central area, a normal stress of 25 MPa was necessary for contact with the central zone only with the LARGE space and gauges of 10 μm. This phenomenon is
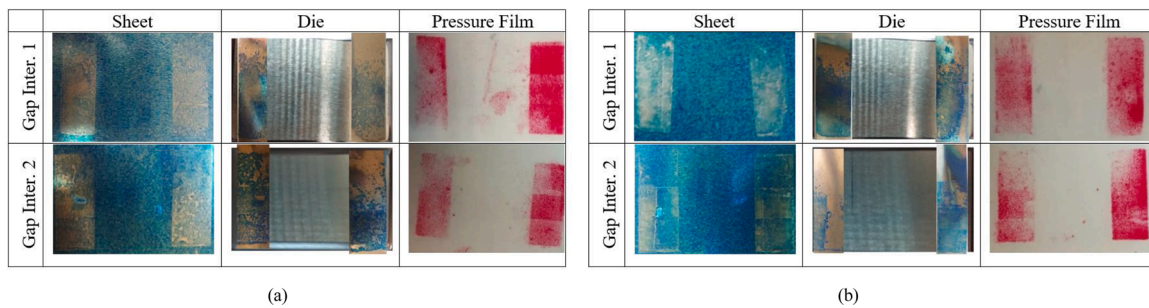
Fig. 10. Gap in both sides/LARGE space between protuberances of 10 microns (a) and 20 microns (b) under 0.5 MPa of apparent contact pressure.
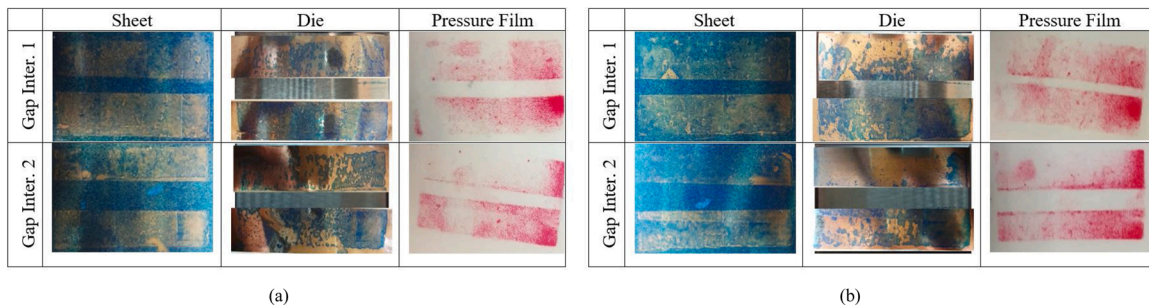

Fig. 11. Gap in both sides/SHORT space between protuberances of 10 microns (a) and 20 microns (b) under 0.5 MPa of apparent contact pressure.
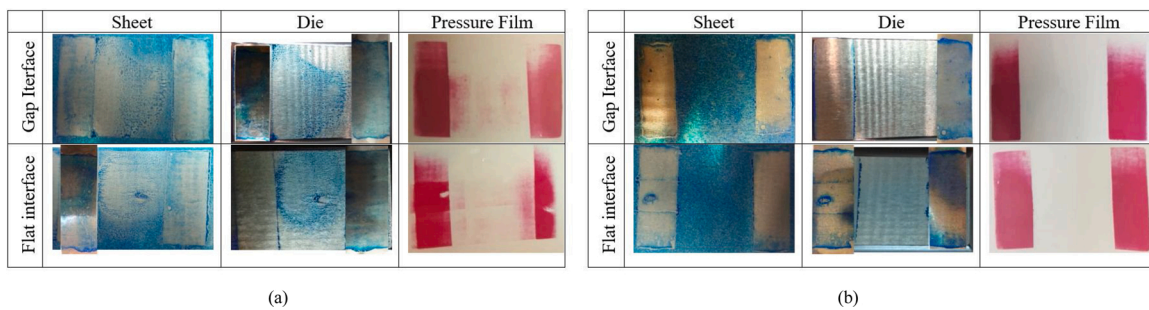

Fig. 12. Gap in both sides/LARGE space between protuberances of 10 microns (a) and 20 microns (b) under 25 MPa of apparent contact pressure.
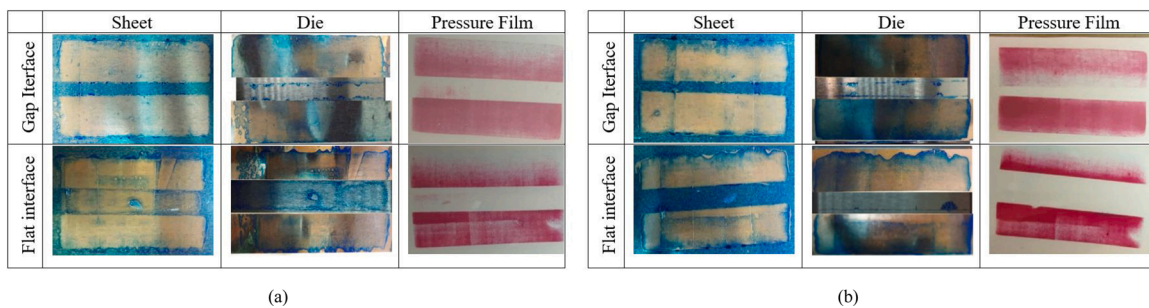

Fig. 13. Gap in both sides/SHORT space between protuberances of 10 microns (a) and 20 microns (b) under 25 MPa of apparent contact pressure.

related to the deformation of the sheet stemming from localised pressure.

This conclusion goes against the general industrial belief that the blue paste pattern is able to exhibit a transfer from sheet to die spaces larger than 10 μm (for a general industrial conclusion, the size of the free space will have to be taken into account). However, it also demonstrates that, even for a blue paste layer of 5 μm, the surrounding contact distribution can force a transfer with gaps lower or equal to 10 μm.

A different factor that should be considered, which was already

mentioned in the previous section, is that the blue paste was pushed out from the 'hard' and 'very hard' local contact areas. In the tests analysed in this work, a critical amount of that blue paste was pushed out of the interface; however, in an industrial die, in which the 'hard contact' area is located in the middle of the die, this pushed out blue paste could lead to a misinterpretation of the surrounding area blue patterns.

Table 6
Occurrence of central gap contact blue paste pattern.

Pressure	Gap (g)	Gap space (h)	N° of gap interfaces	Central contact
0.5 MPa	10 μm	Large	One	YES
0.5 MPa	20 μm	Large	One	NO
0.5 MPa	10 μm	Short	One	NO
0.5 MPa	20 μm	Short	One	NO
25 MPa	10 μm	Large	One	YES
25 MPa	20 μm	Large	One	NO
25 MPa	10 μm	Short	One	YES
25 MPa	20 μm	Short	One	NO
0.5 MPa	10 μm	Large	Both	NO
0.5 MPa	20 μm	Large	Both	NO
0.5 MPa	10 μm	Short	Both	NO
0.5 MPa	20 μm	Short	Both	NO
25 MPa	10 μm	Large	Both	YES
25 MPa	20 μm	Large	Both	NO
25 MPa	10 μm	Short	Both	NO
25 MPa	20 μm	Short	Both	NO

4.3. Irregular contact

As explained in section 3.3, the main objective of the irregular (industrial-flat) contact analysis was the validation of the previously obtained conclusions under real surfaces. In order to do so, the contact pattern evolution of an irregular surface under different pressures is shown in Fig. 14.

It can be noted that, even at low apparent contact pressures of 0.5 MPa, there were some 'hard contact' areas (right and left lines of contact in which both surfaces lost the blue paste) coexisting with 'medium' and 'soft contact' areas and even areas that did not make contact at all. It should also be noted that the blue paste pattern presents a more precise representation of the true contact area evolution, since the pressure film ranges differed from test to test (see Table 2).

When increasing the apparent contact pressure, the same trend is maintained, but all contact is accentuated on degree (Table 5). In addition, speckled blue paste began to increasingly appear as the apparent pressure increased. However, it is hard to determine if this speckled characteristic stemmed from 'very soft contact' or from the blue paste being pushed out on the 'hard contact' area. It can also be observed that the increase in the true contact area was due to the sheet deformation.

As a reference, the blue paste pattern decryption under 5 MPa and 25 MPa apparent contact is illustrated in Fig. 15a and b, respectively.

In both figures, three different types of blue pattern combinations (sheet/die) can be observed. Table 7 summarizes the critical

characteristics of each blue pattern and its contact interpretation.

In Table 8, the decryption of the blue paste pattern of the irregular test condition under 25 MPa contact pressure is shown.

5. Automatic decryption

As the phenomenon of blue paste transfer and its relation with contact pressure was studied in the previous section, in this section, an automatic local contact pressure identification method (Table 5) is developed. The final objective of the study is the analysis of the potential automatic identification of pressure areas to assist in die spotting automatization.

5.1. Theoretical hypothesis

From the previous section, it can be stated that one of the key factors for contact pressure decryption is the amount of blue paste on the sheet and die areas (Fig. 15). Focusing on one specific interface zone, q_s denotes the quantity of blue paste in the sheet and q_d the quantity of blue paste in the die. Assuming that those quantities have a lower value of zero when there is no blue paste and a value of one when the blue paste is at its maximum, the quantity of blue paste that is pushed out of the contact zone can be calculated as:

$$q_{out} = 1 - (q_s + q_d), \tag{1}$$

following the same theory as that in Table 5.

In addition, q_{is} denotes the quantity of blue paste that disappeared from the sheet:

$$q_{is} = 1 - q_s. \tag{2}$$

Considering the conclusions drawn in Fig. 15 and Table 5, the addition of the above two terms can be used as a representative of the local pressure indicator (LPi):

$$LPi = q_{is} + q_{out}. \tag{3}$$

5.2. Numerical implementation of the hypothesis

In order to numerically implement the presented hypothesis, the following steps are necessary.

1 First, pictures of both the sheet and die (hereafter, the sheet picture will be defined as I_s and the die picture as I_d) must be taken.
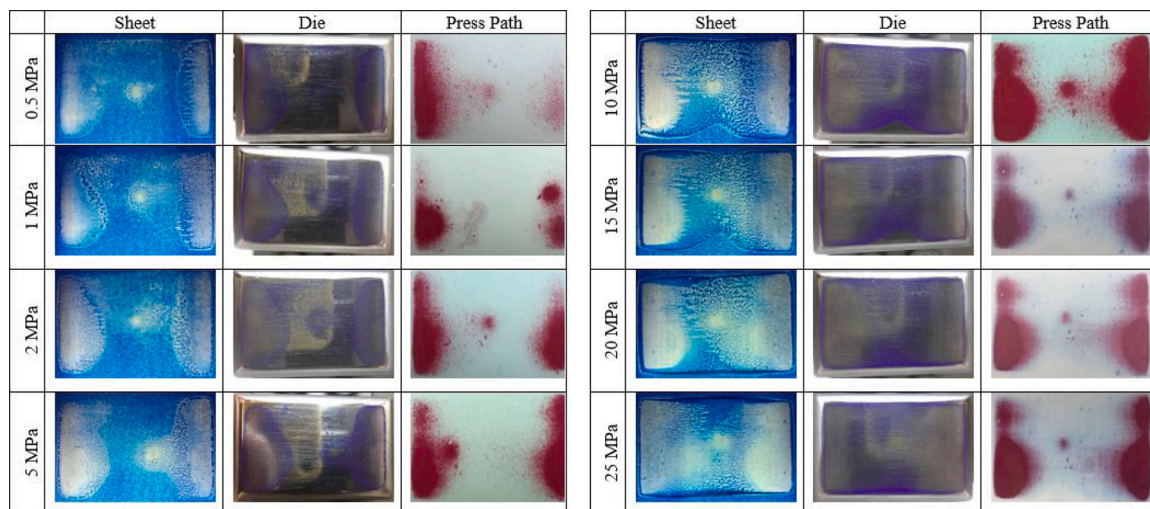
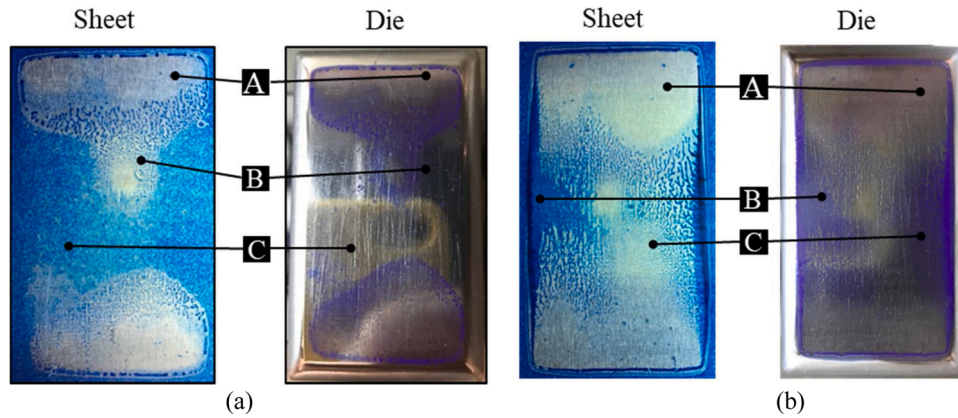**Fig. 14.** Irregular contact under different apparent contact pressures ranging from 0.5 MPa to 25 MPa.

Fig. 15. Decrypted blue paste pattern for irregular test condition under 5 MPa (a) and 25 MPa (b) contact pressure at specified areas referenced as 'A', 'B' and 'C' (For interpretation of the references to colour in this figure legend, the reader is referred to the web version of this article.).

Table 7
Decrypted blue paste pattern for irregular test condition under 5 MPa contact pressure at specified areas referenced as 'A', 'B' and 'C', illustrated in Fig. 15 (reference scale on Table 5).

Point	Sheet blue	Die blue	Speckled	Surrounding effect	Local contact definition
A	NO	NO	–	–	In this case, the pattern combination represents a clear 'hard' *or* 'very hard' (local) contact condition.
B	YES	YES	YES	YES	In this case, the combination represents either a 'soft' *or* 'very soft' (local) contact at the transition between the 'hard contact' and the 'no contact' area. The blue paste on the die could stem from its being pushed out from the 'hard contact'. However, if the latter, no degradation of the colour on the sheet zone was to be expected.
C	YES	NO	–	–	In this case, the combination represents a lack of contact between the faces and, in terms of the surrounding contact pattern, presumably a gap higher than 10 μ.

Table 8
Decrypted blue paste pattern for irregular test condition under 25 MPa contact pressure at specified areas referenced as 'A', 'B' and 'C', illustrated in Fig. 15 (reference scale on Table 5).

Point	Sheet blue	Die blue	Speckled	Surrounding effect	Local contact definition
A	NO	NO	–	–	In this case, the combination represents a clear 'hard' *or* 'very hard' (local) contact condition.
B	YES	YES	NO	NO	In this case, the combination represents 'soft' *to* 'medium' (local) contact.
C	NO	YES	–	–	In this case, the combination represents 'medium' *to* 'hard' (local) contact, as there is still paint on the die area.

2 These pictures must be trimmed to the same area. In this way, the coordinate (x_i, y_i) on the I_s picture corresponds with the local interface of the coordinate (x_i, y_i) on the I_d.

3 Both pictures must then be adjusted to have the exact same number of pixels. By doing this, the pixels of both images can be paired.

4 A representative value of the blue paste intensity of each pixel must then be obtained. In this work, the RGB values of each image are extracted, and, as a quantity indicator, $B/(R \times G)$ has been used. By doing this, it is possible to evaluate the q_s and q_d for every pixel.

5 By applying the calculation presented above, the LPi can be calculated for every pixel.

5.3. Validation of the hypothesis

For validation, the presented numerical implementation was tested for both contact pairs (Fig. 15a and b). Figs. 16 and 17 show the automatic evaluation of the LPi for the 5 MPa and 25 MPa irregular contact cases, respectively.

As can be observed, the proposed methodology is capable of automatically decrypting the combined information from the blue pattern encountered in the sheet (Figs. 16a and 17 a) and die (Figs. 16b and 17 b), thus automatically providing a colour-mapped description of the contact intensities along the contact area (Figs. 16c, Fig. 17c). Based on the previously presented analysis and results (Fig. 15a, b, Table 5), it can be concluded that the proposed automatic methodology can exhibit an accurate trend in local pressure indication. Accordingly, it is presented as a potential tool to be used in objective decision-making towards the automatization of the die spotting process. This methodology will allow for further developing automatic-assisted die spotting for try-out operations.
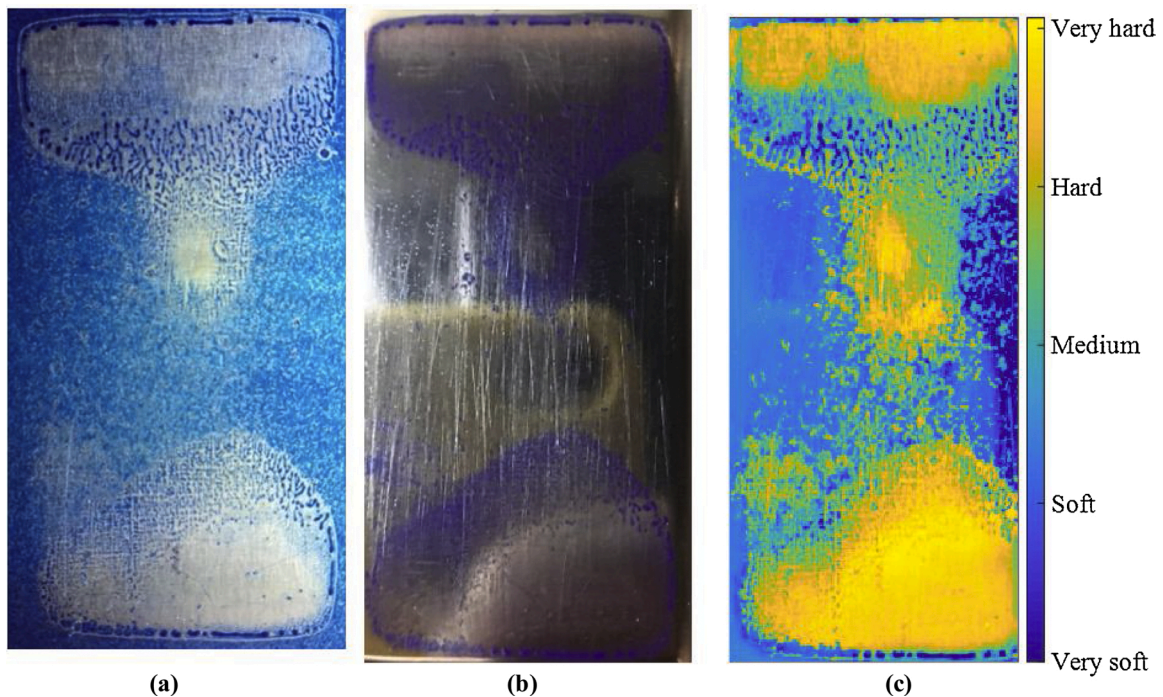
6. Conclusions

In this work, the first steps toward the automatization of spotting were performed via the decryption of the contact blue pattern. To do so, different test procedures were followed, and the evolution of the blue paste pattern for both surfaces of the interface was studied. Additionally, a numerical model for automatic contact detection was developed and validated. The main conclusions that can be drawn from this work include:
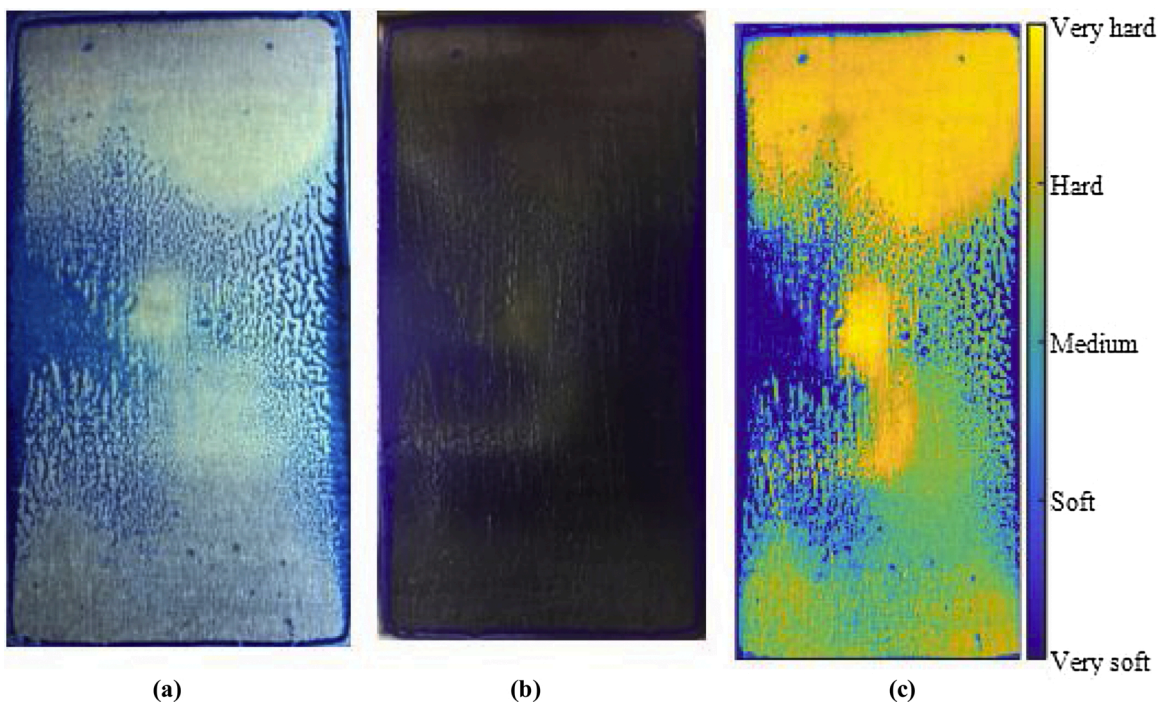
Fig. 16. Decrypted blue-pattern of the 5 MPa contact pressure irregular test via the automatic identification of the pressure areas: a) sheet blue paste pattern image, b) die blue paste pattern image, and c) local pressure indicator (LPi) (For interpretation of the references to colour in this figure legend, the reader is referred to the web version of this article.).

Fig. 17. Decrypted blue paste pattern of the 25 MPa contact pressure irregular test via the automatic identification of the pressure areas: a) sheet blue paste pattern image, b) die blue paste pattern image, and c) local pressure indicator (LPi) (For interpretation of the references to colour in this figure legend, the reader is referred to the web version of this article.).

- A scale ranging 'no-contact' to 'very hard contact' can be addressed depending on the amount of blue paste remaining on both surfaces of the interface. This scale is summarized in Table 5.
- Even if the blue paste pattern on the sheet is reduced when increasing the contact pressure, the pattern follows a concave trend on the die at

- a maximum of around 5 MPa. At higher pressures, the blue paste is squeezed out of the interface.
- This squeezing the blue paste under high pressures could lead to misguidance in the surrounding areas in some cases.
- Even if the initial blue paste layer on the top of the sheet is around 5 μm, the local deformation of the sheet due to the surrounding high

local pressures could lead to blue paste transfer with gaps of 10 μm on the interface (20 μm is estimated as the maximum value of the gap that allows transferring under the analysed conditions).

- The developed numerical methodology disclosed a good correlation with the contact intensities along the contact area

The outcome of this study is presented as a potential tool to be used in objective decision-making towards the automatization of the die spotting process and die contact analysis, with the aim of decreasing try-out loops and thus reducing production costs. Future challenges to be addressed includes the study of more complex real tool shapes (and industrially relevant part sizes) that include sliding phenomena, as well as the impact of the material type of the tribosystem in the blue paste transfer behaviour.

Declaration of Competing Interest

The authors report no declarations of interest.

Acknowledgments

References

[1] Roth R, Clark J, Kelkar A. Automobile bodies: Can aluminum be an economical alternative to steel? JOM 2001;53:28–32. https://doi.org/10.1007/s11837-001-0131-7.

[2] Ficko M, Drstvenšek I, Brezočnik M, Balič J, Vaupotic B. Prediction of total manufacturing costs for stamping tool on the basis of CAD-model of finished product. J Mater Process Technol 2005;164–165:1327–35. https://doi.org/10.1016/j.jmatprotec.2005.02.013.

[3] Schuh G, Pitsch M, Komorek N, Schippers M, Salmen M. Cutting manufacturing failure costs in the tool and die industry by implementing a knowledge transfer system to avoid and correct mistakes more effectively. Procedia CIRP 2014;16:80–5. https://doi.org/10.1016/j.procir.2014.02.002.

[4] Birkert Arndt, Haage Stefan, MS. Umformtechnische Herstellung Komplexer Karosserieteile. Berlin, Heidelberg: Springer Berlin Heidelberg; 2013. https://doi.org/10.1007/978-3-642-34670-5.

[5] Wei L, Yuying Y, Zhongwen X, Lihong Z. Springback control of sheet metal forming based on the response-surface method and multi-objective genetic algorithm. Mater Sci Eng A 2009;499:325–8. https://doi.org/10.1016/j.msea.2007.11.121.

[6] Mendiguren J, Cortés F, Galdos L, Berveiller S. Strain path's influence on the elastic behaviour of the TRIP 700 steel. Mater Sci Eng A 2013;560:433–8. https://doi.org/10.1016/j.msea.2012.09.087.

[7] Banabic D. Sheet metal forming processes. Berlin, Heidelberg: Springer Berlin Heidelberg; 2010. https://doi.org/10.1007/978-3-540-88113-1.

[8] Neuhauser FM, Terrazas O, Manopulo N, Hora P, Van Tyne C. The bending dependency of forming limit diagrams. Int J Mater Res 2019;12:815–25. https://doi.org/10.1007/s12289-018-1452-1.

[9] Wang C, Ma R, Zhao J, Zhao J. Calculation method and experimental study of coulomb friction coefficient in sheet metal forming. J Manuf Process 2017;27:126–37. https://doi.org/10.1016/j.jmapro.2017.02.016.

[10] Weikert T, Tremmel S, Stangier D, Tillmann W, Krebs E, Biermann D. Tribological studies on multi-coated forming tools. J Manuf Process 2020;49:141–52. https://doi.org/10.1016/j.jmapro.2019.11.021.

[11] Sigvant M, Pilthammar J, Hol J, Wiebenga JH, Chezan T, Carleer B, et al. Friction and lubrication modeling in sheet metal forming simulations of a Volvo XC90 inner door. IOP Conf Ser Mater Sci Eng 2016;159. https://doi.org/10.1088/1757-899X/159/1/012021.

[12] Tatipala S, Pilthammar J, Sigvant M, Wall J, Johansson CM. Introductory study of sheet metal forming simulations to evaluate process robustness. IOP Conf Ser Mater Sci Eng 2018;418. https://doi.org/10.1088/1757-899X/418/1/012111.

[13] Sigvant M, Pilthammar J, Hol J, Wiebenga JH, Chezan T, Carleer B, et al. Friction in sheet metal forming: influence of surface roughness and strain rate on sheet metal forming simulation results. Procedia Manuf 2019;29:512–9. https://doi.org/10.1016/j.promfg.2019.02.169.

[14] Merklein M, Andreas K, Steiner J. Influence of tool surface on tribological conditions in conventional and dry sheet metal forming. Int J Precis Eng Manuf - Green Technol 2015;2:131–7. https://doi.org/10.1007/s40684-015-0017-8.

[15] Arumugaprabu V, Ko TJ, Thirumalai Kumaran S, Kurniawan R, Uthayakumar M. A brief review on importance of surface texturing in materials to improve the tribological performance. Rev Adv Mater Sci 2018;53:40–8. https://doi.org/10.1515/rams-2018-0003.

[16] Shisode MP, Hazrati J, Mishra T, de Rooij MB, van den Boogaard AH. Semi-analytical contact model to determine the flattening behavior of coated sheets under normal load. Tribol Int 2020;146:106182. https://doi.org/10.1016/j.triboint.2020.106182.

[17] Pilthammar J, Sigvant M, Hansson M, Pálsson E, Rutgersson W. Characterizing the elastic behaviour of a press table through topology optimization. J Phys Conf Ser 2017:896. https://doi.org/10.1088/1742-6596/896/1/012068.

[18] Pilthammar J, Sigvant M, Kao-Walter S. Introduction of elastic die deformations in sheet metal forming simulations. Int J Solids Struct 2018;151:76–90. https://doi.org/10.1016/j.ijsolstr.2017.05.009.

[19] Recklin V, Dietrich F, Groche P. Influence of test stand and contact size sensitivity on the friction coefficient in sheet metal forming. Lubricants 2018:6. https://doi.org/10.3390/lubricants6020041.

[20] Bolay C, Essig P, Kaminsky C, Hol J, Naegele P, Schmidt R. Friction modelling in sheet metal forming simulations for aluminium body parts at Daimler AG. IOP Conf Ser Mater Sci Eng 2019:651. https://doi.org/10.1088/1757-899X/651/1/012104.

[21] Leocata S, Senner T, Saubiez JM, Brosius A. Influence of binder pressure zones on the robustness of restraining forces in sheet metal forming. Procedia Manuf 2019;29:209–16. https://doi.org/10.1016/j.promfg.2019.02.128.

[22] Essig P, Liewald M, Bolay C, Schubert T. Digital process support in toolmaking by using optical metrology. IOP Conf Ser Mater Sci Eng 2019:651. https://doi.org/10.1088/1757-899X/651/1/012026.

[23] Koch S, Behrens B-A, Hübner S, Scheffler R, Wrobel G, Pleßow M, et al. 3D CAD modeling of deep drawing tools based on a new graphical language. Comput Aided Des Appl 2018;15:619–30. https://doi.org/10.1080/16864360.2018.1441228.

[24] Gil I, Mendiguren J, Galdos L, Mugarra E, Saenz de Argandoña E. Influence of the pressure dependent coefficient of friction on deep drawing springback predictions. Tribol Int 2016;103:266–73. https://doi.org/10.1016/j.triboint.2016.07.004.

[25] ASTM D1212 - 91-Standard test methods for measurement of wet film thickness of organic coatings. 2013.